การสังเคราะห์ ศึกษาโครงสร้าง การคำนวณโดยใช้ทฤษฎีฟังก์ชันนอลความหนาแน่น และความเป็นพิษต่อเซลล์มะเร็งเต้านมในหลอดทดลองของสารประกอบเชิงซ้อน Ru(*p*-cymene)(PPh_3)Cl_2

Synthesis, Characterization, Theoretical Calculation-Based Density Functional Theory and *In vitro* Cytotoxicity Against Breast Cancer Cell Lines of Ru(*p*-cymene)(PPh_3)Cl_2 Complex

Vannara Some [1] ธมลวรรณ ส่องแสง [1] เอกพงษ์ คล้ายมณี [1] ฐิติรัตน์ เต็มราม [1] เสาวนิต ทรายทอง [1]
อดิศร รัตนพันธ์ [2] และ นรารักษ์ หลีสกุล [1*]
Vannara Some [1], Thamolwan Songsan [1], Ekkapong Klaimanee [1], Thitirat Temrarm [1], Saowanit Saithong [1], Adisorn Ratanaphan [2] and Nararak Leesakul [1*]
Received: 24 March 2023, Revised: 3 May 2023, Accepted: 2 June 2023

บทคัดย่อ

เป็นที่ทราบกันดีว่าสารประกอบเชิงซ้อนของโลหะรูทีเนียม เป็นสารที่มีความสำคัญและมีความเป็นไปได้ในการยับยั้งการเจริญเติบโตของเนื้องอก และเซลล์มะเร็ง ในงานวิจัยนี้ Ru(*p*-cymene)(PPh_3)Cl_2 ถูกสังเคราะห์ผ่านปฏิกิริยาการแทนที่ระหว่างไดเมอร์ของสารประกอบเชิงซ้อน dichloro(*p*-cymene)ruthenium(II) กับลิแกนด์ไตรฟีนิลฟอสฟีน (PPh_3) ในตัวทำละลายไดคลอโรมีเทน เพื่อใช้ในการศึกษาการออกฤทธิ์ยับยั้งการเจริญเติบโตของเซลล์มะเร็งเต้านมในหลอดทดลอง ศึกษาโครงสร้างของสารประกอบเชิงซ้อนดังกล่าวด้วยเทคนิค Single crystal X-ray diffraction, ^{1}H-NMR, FTIR และการวิเคราะห์ปริมาณธาตุที่เป็นองค์ประกอบ พบว่าสารประกอบเชิงซ้อนชนิดนี้มีโครงสร้างเป็นทรงเหลี่ยมสี่หน้าบิดเบี้ยว (distorted tetrahedral) โดยศึกษาเคมีคำนวณภายใต้ทฤษฎีฟังก์ชันนอลความหนาแน่น (density functional theory) เพื่อใช้ในการอธิบายคุณลักษณะของแถบการดูดกลืนแสงที่ความยาวคลื่นของการดูดกลืนแสงสูงสุดที่ 393 นาโนเมตร และมีไหล่ (shoulder) ของแถบการดูดกลืนที่ 496 นาโนเมตร เมื่อเกิดจากการเปลี่ยนระดับพลังงานจากการถ่ายโอนประจุ (charge transfer) และศึกษาความเป็นพิษของสารประกอบเชิงซ้อน Ru(*p*-cymene)(PPh_3)Cl_2 กับเซลล์มะเร็งเต้านม จำนวน 3 ชนิด ได้แก่ HCC1937 MCF-7 และ MDA-MB-231 โดยวิธี MTT assay พบว่าสารประกอบชนิดนี้ออกฤทธิ์ยับยั้งการเจริญเติบโตของเซลล์ MCF-7 ให้ค่า IC_{50} เท่ากับ 15.99 μM ดีกว่าสาร cisplatin (42.2 μM) ซึ่งเป็นยาทางการค้าถึง 2.6 เท่า

---

[1] สาขาวิทยาศาสตร์กายภาพ คณะวิทยาศาสตร์ มหาวิทยาลัยสงขลานครินทร์ อำเภอหาดใหญ่ จังหวัดสงขลา 90110
[1] Division of Physical Science and Center of Excellence for Innovation in Chemistry, Faculty of Science, Prince of Songkla University, Hat Yai, Songkhla 90110, Thailand.
[2] ภาควิชาเภสัชเคมี คณะเภสัชศาสตร์ มหาวิทยาลัยสงขลานครินทร์ อำเภอหาดใหญ่ จังหวัดสงขลา 90110
[2] Department of Pharmaceutical Chemistry, Faculty of Pharmaceutical Sciences, Prince of Songkla University, Hat Yai, Songkhla 90112, Thailand.
[*] Corresponding author, e-mail: nararak.le@psu.ac.th Tel: 0 7428 8421

คำสำคัญ: สารประกอบเชิงซ้อนโลหะรูทีเนียม(II), ไตรฟีนิลฟอสฟีน, ทฤษฎีฟังก์ชันนอลความหนาแน่น, ฤทธิ์ต้านมะเร็ง

ABSTRACT

Ruthenium complexes are known as promising crucial substances for *in vitro* antitumor and anticancer. In this study, Ru(*p*-cymene)(PPh_3)Cl_2 was synthesized through a consequence reaction between dichloro(*p*-cymene)ruthenium(II) dimer and triphenylphosphine (PPh_3) ligand in dichloromethane to investigate its in vitro activity against breast cancer cells comparison with free PPh_3 ligand. The complex was characterized using single crystal X-ray diffraction, ^{1}H-NMR, FTIR, elemental to analyze its specific structure which adopted a distorted pseudo-tetrahedral geometry. Theoretical calculations under density functional theory were conducted to identify that the absorption band at 393 nm with a shoulder of 496 nm arose from the characters of charge transfer transitions. The Ru(p-cymene)(PPh_3)Cl_2 complex was measured for cytotoxicity against three breast cancer cell lines, HCC1937, MCF-7, and MDA-MB-231 by MTT assay. It exhibited higher anti-breast cancer activity against MCF-7, with an IC50 value of 15.99 µM, compared to cisplatin, a commercial drug (42.2 µM), by 2.6 folds.

Key words: ruthenium(II) complex, triphenylphosphine, density functional theory, anticancer

INTRODUCTION

In recent years, scientists have tried to explore chemotherapeutic drugs' resistance to cancer cells, and they remain ineffective in treating many diverse types of cancer (Pettinari *et al.*, 2014). The primary motivation for research to develop new metallodrugs with anticancer efficacy is the discovery of novel metallodrugs (Rojas *et al.*, 2017). Currently, there has been a lot of pharmacological interest in organometallic Ru(II) complexes based on the arene complex because of their antitumor, anticancer, and antibacterial activities (Yellol *et al.*, 2015; Lapasam *et al*., 2019). Compared to platinum-based drugs like cisplatin, the half-sandwich *p*-cymene-ruthenium(II) complexes from a piano stool show anticancer efficacy with low toxicity to normal cells (Subarkhan and Ramesh, 2016; Brissos *et al*., 2018). Ruthenium-based drugs exhibit stronger anticancer effects within the same activity spectrum as Pt(II) based drugs, which is possibly explained by their capacity to mimic iron, trigger apoptosis, and bind to DNA, proteins, and enzymes (Allardyce and Dyson, 2001; Bergamo and Sava, 2011; Neethu *et al*., 2019). The main way that the synthesis of anticancer ruthenium(II) complexes has been developed recently is by altering the N-donor, O-donor, S-donor, and P-donors of auxiliary ligands (Brissos *et al.*, 2018; Rohini *et al.*, 2018; Orhan *et al.*, 2022). However, most researchers have concentrated on Ru-arene structures with N-donor ligands (Dkhar *et al.*, 2020). Additionally, phosphine derivatives can interact with DNA chain. RAPTA-C is a Ru(II) complex consisting of the bond between Ru(II) with an arene group, two chloro ligands, and a phosphorus donor as an ancillary ligand (Herry *et al.*, 2019). It has been found that RAPTA-C plays an important role as an anticancer agent (Murray *et al.*, 2016). Many researchers have reported phosphine- derived complexes containing Ru(II) metal ions with mononuclear structural geometry (Biancalana *et al.*, 2017) similar to our group's work (Chuklin *et al.*, 2017; Klaimanee *et al*., 2021) as well as some small number of P^P chelating ligands of bimetallic Ru(II) complexes (Herry *et al.*, 2019). Some other strong anticancer properties of Ru(II) and Ir(III) complexes with P^P ligands were reported by Li and coworkers. The Ru(II) complexes [η^6-*p*-cym)Ru(P^P) Cl]PF_6 (BINAP) exhibited potent anticancer activity up to 15 and 7.5 times greater than

cisplatin, respectively, against A549 and HeLa cells (Li *et al.*, 2018). There are many mechanisms for explaining the anti-growth of cancer cells by Ru(II) complexes for example, cellular uptake, interaction with nucleic acids and proteins through multiple binding modes in the nucleus, interaction on mitochondria, lysosome, DNA, and enzymes (Zeng *et al.*, 2017). In addition, the Ru(II) complexes with P-donor ligands have been also widely investigated for their antimicrobial activities (Mawnai *et al*., 2019).

In this present work, the piano-stool structure of a simple molecule was synthesized and characterized by single crystal X-ray diffraction, spectroscopies, and elemental analysis. This complex has been reported by Elsegood and coworkers before, but it has never been revealed its intra- and inter-molecular force and Hirshfield surface stucture interactions yet. Moreover, Honorato and coworkers have also studied the cytotoxicity of this complex against many kinds of cancer cells. Nevertheless, its anticancer property against the HCC1937 human breast cancer cell line has not yet been studied. Besides, the in-depth understanding of the optical property of this complex has also never been reported. Herein, we report all those missing points together with the theoretical calculations based on DFT to stimulate the absorption spectrum in CH_2Cl_2 which are new aspects to be explored. The Ru(*p*-cymene)(PPh_3)Cl_2 is aimed to be used as a precursor for synthesizing the [Ru(*p*-cymene)(PPh_3)L]Cl complex where L = various types of amino acids for the anticancer framework. Therefore, a well-understand chemistry of the precursor complex is essential.

MATERIALS AND METHODS

Materials

The A.R. grade of dichloro(*p*-cymene) ruthenium(II) complexes dimer and triphenylphosphine were purchased from TCI. Reagent-grade solvents, such as chloroform, dichloromethane, acetonitrile, and diethyl ether, were bought from RCI Labscan. No extra purification was done and used as received.

Instrumentation

A BX Perkin Elmer FT-IR spectrophotometer (KBr disk, 4000-400 cm^{-1}) was used to record the vibrational frequency spectra of the complex. A Varian Bruker Avance 300 MHz NMR spectrometer was used to perform proton nuclear magnetic resonance (^{1}H-NMR) spectra in $CDCl_3$ solvent with tetramethyl silane (TMS) as an internal standard. The absorption spectra of the studied complex were measured using a UV-visible spectrophotometer, model TU-1950, to record electronic spectra (200-800 nm). The visible and ultraviolet light sources were provided by tungsten and deuterium lamps, respectively. A standard 1 cm quartz cuvette was used. The Electrothermal IA9000 Series melting point instrument was used to measure melting points. Elemental analysis was conducted using a CHNS-O Analyzer, (CEv Instruments Flash EA 1112 Series, Thermo Quest, Italy). The diffraction data of Ru(*p*-cymene)(PPh_3)Cl_2 complex were collected using a D8 VENTURE Bruker AXS apparatus with graphite-monochromated Mo Kα radiation (λ = 0.71073 Å). The diffraction data of were collected from 30304 reflections. The interpretation of raw data was obtained using SMART, SAINT v8.38A, and SADABS software. Structure solving was carried out using SHELXS (Sheldrick, 2015). Non-hydrogen atoms were refined from anisotropic thermal parameters. A riding model was used to refine calculations with all hydrogen atoms placed in ideal positions. Molecular graphics and materials required for publication were prepared by the WinGX 2018/3 (Farrugia, 2012) and Mercury 2020.3 (MacRae *et al.*, 2020) programs. Crystallographic data for Ru(*p*-cymene)(PPh_3)Cl_2 were deposited at the Cambridge Crystallographic Data Center and can be provided using the access CCDC code 2231646, via: http://www.ccdc.cam.ac.uk/data request/cif (or from the Cambridge Crystallographic Data Centre, 12 Union Road, Cambridge CB21EZ, U.K. Fax: +44 1223 336 033 or email deposit@ccdc.cam.

ac.uk). The X-ray data were provided in the supplementary data section.

Synthesis pathway

The Ru(*p*-cymene)(PPh_3)Cl_2 complex was prepared by reacting dichloro(*p*-cymene) ruthenium(II) dimer (0.183g, 0.3 mmol) with triphenylphosphine (PPh_3) (0.157g, 0.6 mmol) ligand in 20 mL of tetrahydrofuran (THF) at 40ºC. The mixture of these substances was stirred for 1.5 hours. After that, the compounds were filtered and crystallized by adding dichloromethane and acetonitrile 2: 1 ratio, followed by diffusion of vapor with diethyl ether (10 mL), and left at room temperature for a few days to obtain single crystals. The obtained brown single crystals were filtered and washed with diethyl ether three times. Moreover, the complex was recrystallized again in the same solvent mixture. The complex crystals were completely soluble in dichloromethane and $CDCl_3$.

Yield: 61.86%. Melting point: 194-195ºC (with decomposition). Anal Calcd (%) for $C_{28}H_{29}Cl_2PRu$ (568.45), C 59.10, H 5.10, Found, C 58.99, H 5.07. FT-IR (KBr, cm^{-1}) see supplementary data Figure S1: υ(C-H), 3049; υ(C = C), 1436; υ(P-Ph), 1092; υ(Ru-P), 525; υ(Ru-Cl), 508 cm^{-1}. ^{1}H-NMR (300 MHz, $CDCl_3$) see supplementary data Figure S2: δ 7.82 (dd, J = 7.5Hz, 6H), 7.38 (d, J = 7.5Hz, 9H), 5.19 (d, J =7.5 Hz, 2H), 4.99 (d, J = 7.5 Hz, 2H), 2.85 (m, J = 6.8 Hz, 1H), 1.87 (s, 3H) and 1.10 (d, J = 6.8 Hz, 6H)

Computational study

The Gaussian 09 program was used for all calculations. The calculation was done based on the density functional theory (DFT) in the gas phase with PBE0 (Tabares *et al.*, 2019) and B3LYP basis sets (Klaimanee *et al.*, 2021). The ground state of the Ru(II) complex was completely optimized in terms of shape. For non-metal atoms and the ruthenium atom, the basis sets of 6-31G(d) and LANL2DZ were selected, respectively (Roy *et al.*, 2008). The electronic absorption spectrum was then simulated by using the TDDFT program and the polarizable continuum model (PCM) of dichloromethane (Mennucci *et al.*, 1997).

***In vitro* cytotoxicity assay**

The MTT assay was used to measure the anti-breast cancer activity against the MCF-7, MDA-MB-231, and HCC1937 cell lines. Cisplatin was used as a positive control to assess the complex's cytotoxicity against breast cancer cells. The IC_{50} value of Ru(*p*-cymene)(PPh_3)Cl_2 complex was reported. Human breast adenocarcinoma cell line (ATCC® HTB-22™) was [MCF-7 breast cancer (BRCA1 wild-type, ER-, PR-, and HER2-positive)] (ATCC, USA). Human breast adenocarcinoma cell line (ATCC® HTB-26™) was [MDA-MB-231 breast cancer (BRCA1 wild-type, Triple negative (ER-, PR-, and HER2-negative)] (ATCC, USA). The human breast adenocarcinoma cell line (ATCC® CRL-2336™) was [HCC1937 breast cancer (BRCA1 mutant, Triple negative (ER-, PR-, and HER2-negative)] (ATCC, USA).

RESULTS AND DISCUSSION

Synthesis and characterization

The complex, Ru(*p*-cymene)(PPh_3)Cl_2 was synthesized by a new method involving between dichloro(*p*-cymene) ruthenium(II) dimer complexes and triphenylphosphine (PPh_3) ligand in tetrahydrofuran (Scheme 1).

The results from single-crystal XRD, FT-IR, ^{1}H-NMR, and elemental analysis techniques were examined to confirm the structure of Ru(*p*-cymene)(PPh_3)Cl_2 complex, which adopted a distorted pseudo-tetrahedral geometry with η^6 π-bonding of *p*-cymene, a single molecule of triphenylphosphine (PPh_3), and two Cl^- ligands (Figure 1). The crystallographic information for the Ru(*p*-cymene)(PPh_3)Cl_2 complex is displayed in Supplementary data T1 and T2. The crystal structure of the Ru(*p*-cymene)(PPh_3)Cl_2 complex is monoclinic with the $P2_1/n$ space group, reported in a previous study (Elsegood *et al.*, 2006). The selected bond distances (Å) and bond angles (º) of the Ru(*p*-cymene)(PPh_3)Cl_2 complex are displayed in supplementary data

T3. There are two molecules in the asymmetric unit (the label Ru(1) and Ru(2) for molecules 1 and 2, respectively). The averaged distances of Ru-P 2.3488(5) Å, Ru-Cl 2.4133(6) Å, and averaged Ru-C 2.219(2) Å distances are close to the previously studied by Elsegood *et al.* (2006). These results are similar to other related structures of [(η^6-*p*-cymene)]$RuCl_2(PPh_2Py)$] (Govindaswamy *et al.*, 2004) and [Ru_2(*p*-cymene)$_2$(dppp)Cl_4] complexes (Klaimanee *et al.*, 2021). The bond angles of P(1)-Ru(1)-Cl(1), P(1)-Ru(1)-Cl(2), and Cl(1)-Ru(1)-Cl(2) of the complex are 90.21(2)°, 87.112(19)°, and 88.46(2)° for molecule 1 and P(2)-Ru(2)-Cl(4), P(2)-Ru(2)-Cl(3), and Cl(1)-Ru(1)-Cl(2) in the complex are 87.62(2)°, 89.81(2)°, and 88.81(2)° for molecule 2, respectively. This points out that our studied complex is pseudo-tetrahedral or distorted tetrahedral in both molecules, similar to earlier studies (Elsegood *et al.*, 2006; Ludwig *et al.*, 2012). Weak intramolecular H-bonding of C-H---Cl types is found between H atoms of the phenyl ring of PPh_3 and Cl atoms in the crystal structure of the Ru(*p*-cymene)(PPh_3)Cl_2 complex (Figure 2 and Table 1). In addition, an intermolecular force between molecule 2 of C-H···π of C(47)-H(47)···*Cg8* = 2.81 Å is presented, as shown in Figure 3 and Figures S3-S4 (Supplementary data).

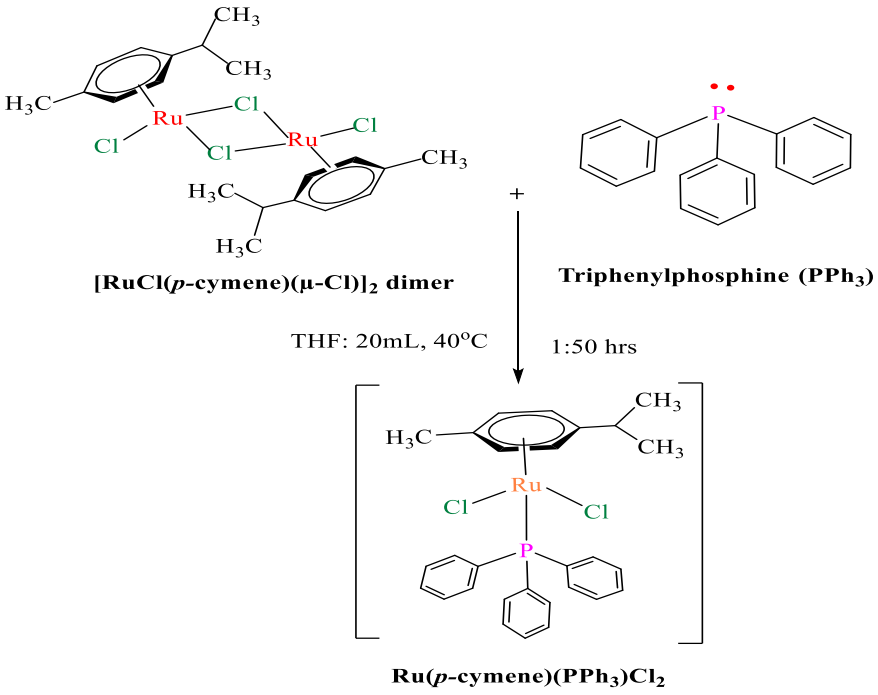

Scheme 1 Synthesis pathway of Ru(*p*-cymene)(PPh_3)Cl_2 complex.

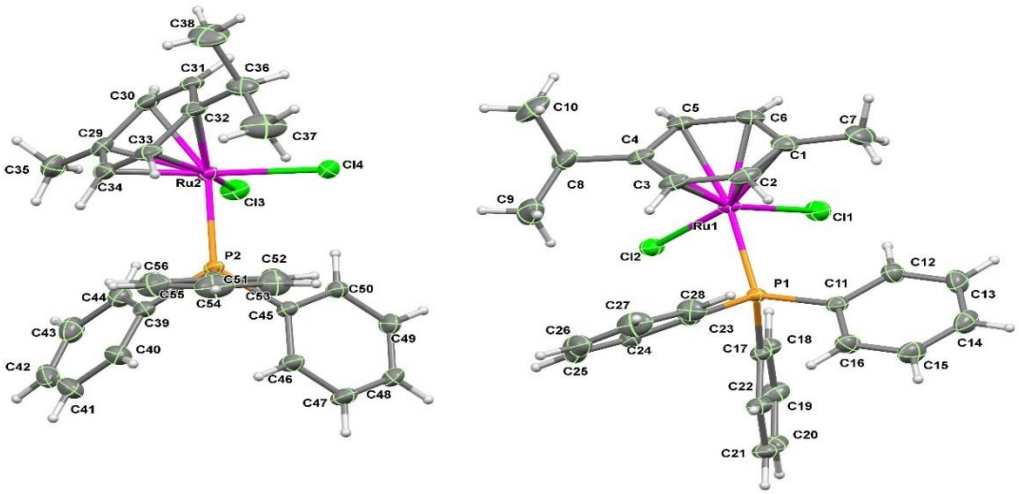

Figure 1 The ORTEP structures of Ru(*p*-cymene)(PPh_3)Cl_2 complex in asymmetric unit with atom numbering

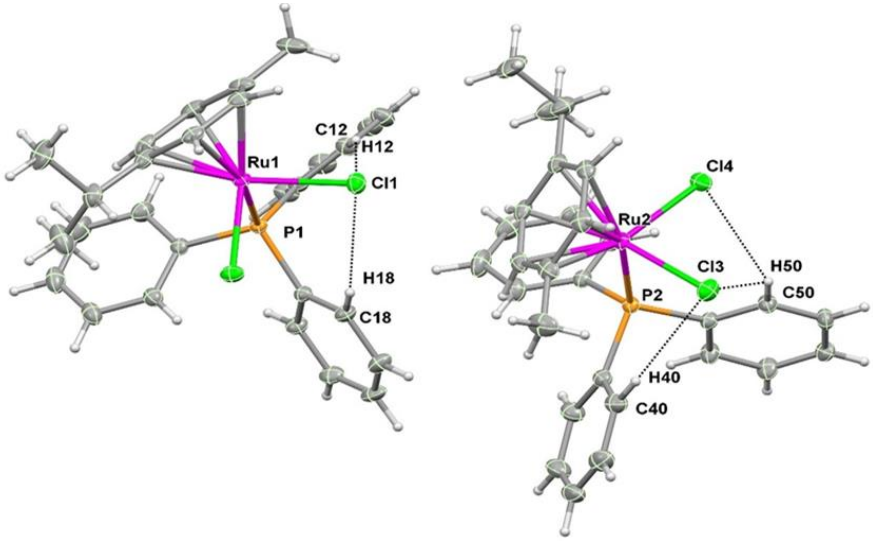

Figure 2 The intra-molecular hydrogen bond interactions of Ru(*p*-cymene)(PPh_3)Cl_2 complex

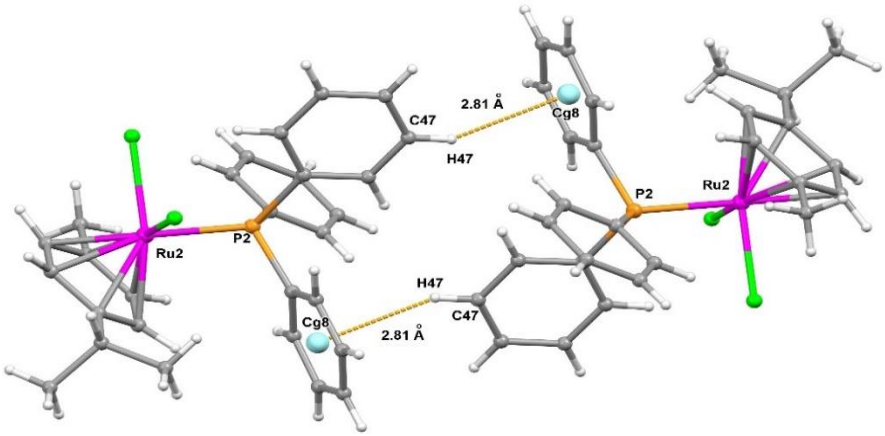

Figure 3 Inter-molecular C-H···π interactions of Ru(*p*-cymene)(PPh_3)Cl_2 complex.

Table 1 Hydrogen bonds for Ru(*p*-cymene)(PPh_3)Cl_2 complex[Å, º].

D-H...A	Distance of d(D-H) (Å)	Distance of d(H...A) (Å)	Distance of d(D...A) (Å)	Angles of <(DHA) (º)
C(12)-H(12)...Cl(1)	0.93	2.74	3.564(3)	147.9
C(18)-H(18)...Cl(1)	0.93	2.71	3.476(3)	140.1
C(40)-H(40)...Cl(3)	0.93	2.71	3.548(3)	149.7
C(50)-H(50)...Cl(3)	0.93	2.72	3.435(2)	134.2
C(50)-H(50)...Cl(4)	0.93	2.72	3.295(2)	121.1

Symmetry transformations are used to generate equivalent atoms.

Hirshfeld surface analysis

Hirshfeld surface analysis was used to examine the intermolecular interactions in the crystal packing. Hirshfeld surfaces mapped over d_{norm} were created using the Crystal Explorer program (Spackman *et al.*, 2021). The intermolecular contact distances, d_i and d_e, from the surfaces between the closest atoms inside and outside molecules were analyzed using the mapping of d_{norm}. Figure 4 displays a map of the Hirshfeld surfaces over d_{norm} that reveals the intermolecular contacts as acceptors on the surfaces. These contact ratio, followed by diffusion of acts, which are shorter than Van der Waals radii, are represented by bright-red spots on surfaces indicating intermolecular contacts of H···H, C···H/H···C, and H···Cl/Cl···H, respectively. The strong red spots the surface of H48---H25 and H20···H53 of molecule 1 (refer to Ru1) correlate with the H···H short contacts while the surfaces of C6···H10B/H10B···C6 and C25···H21/H21···C25 are the C···H/H···C interactions. For the H···H short contacts of molecule 2 (Ru2) are indicated with H20···H53, H25···H48 and H42···H52. The reciprocal interactions of C ··· H/ H ··· C intermolecular contacts are shown with C30···H38C/H38C···C30, C42···H52/H52···C42. The percentage contribution of the individual types of interactions to the total Hirshfeld surface area is displayed by the 2D fingerprint plots in supplementary data Figure S5 for molecule 1 (Ru1). The crystal packing H···H contacts represent the largest percentage of the Hirshfeld surface with 64.4% with the characteristic wings of 2D fingerprint plots indicating the C–H···π interactions in crystal packing, referring to the C ··· H/ H ··· C interactions with 21.7%. The 12.5% contribution from the H···Cl/Cl···H contacts is the result of the C−H···Cl interactions. The fingerprint plot of molecule 2 (Ru2) depicted in supplementary data Figure S6 is quite similar to that of molecule 1. The 2D fingerprint plot suggests that the intermolecular H··· H contacts have the highest contribution (64.5 %), while the relative contributions of the C···H/H···C and H···Cl/Cl···H contacts are 21.4 % and 12.6 %, respectively.

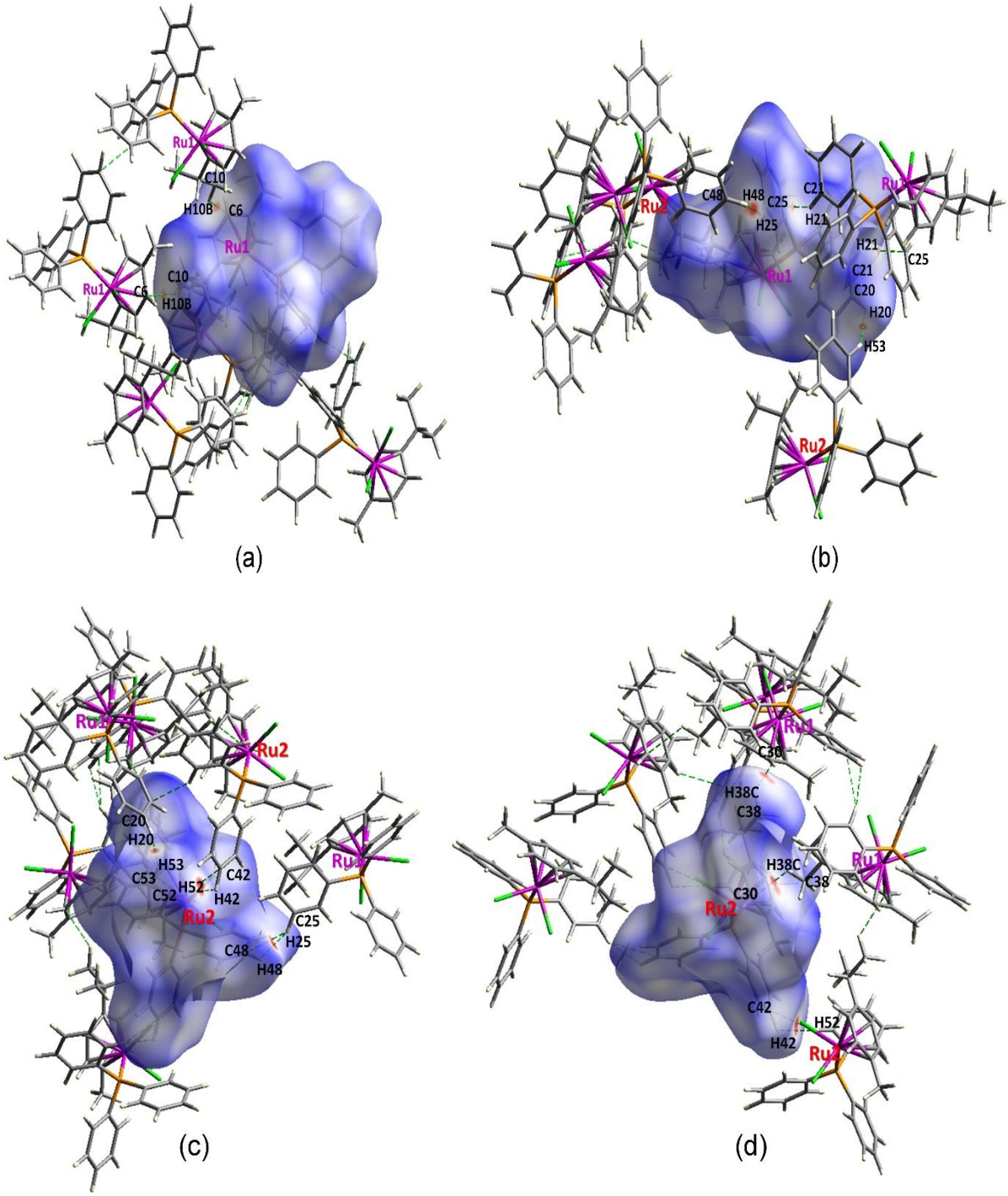

Figure 4 The intermolecular contacts of molecule 1 surfaces (a and b) and molecule 2 surfaces (c and d) with its neighbors for the Ru(*p*-cymene)(PPh_3)Cl_2 complex.

Absorption

The data from the photophysical study and vertical electronic transitions calculated were presented in Table 2 and supplementary data Figure S7. The absorption spectrum of the Ru(*p*-cymene)(PPh_3)Cl_2 complex shows three maximum absorption bands at wavelengths (with molar extinction coefficient) of 228 nm (8.0×10^4 $M^{-1}cm^{-1}$), 373 nm (4.3×10^3 $M^{-1}cm^{-1}$) and 496 nm (1.2×10^3 $M^{-1}cm^{-1}$), respectively. To interpret the electronic transitions yielding the absorption bands, the polarizable continuum model (PCM) of dichloromethane was used to

simulate the electronic absorption spectrum using time-dependent on density functional theory (TDDFT).ThePCM-TD-PBE0/6-31+G*+LANL2DZ basis sets were used for the calculation. The electronic transitions of Ru(*p*-cymene)(PPh_3)Cl_2 complex is shown as vertical lines in Figure 5 aligning to the experimental absorption spectrum. The main transitions regarding those three absorption bands arise from charge transfer transition. The band at 496 nm is belong to ligand-to-ligand charge transfer transition (LLCT) from PPh_3 to *p*-cymene moiety giving HOMO→LUMO (79%) transition ($\lambda_{calc.}$ = 516 nm, Osc. Strength (f) = 0.0084). The HOMO→L+1 (65%) transition is shown by the band at 373 nm ($\lambda_{calc.}$ = 395 nm, Osc. Strength (f) = 0.0213), with mixed MLCT (d-Ru(1)→π*-P(PPh_3) and XLCT (Cl→π*-P(PPh_3) halogen to ligand charge transfer as shown in Figure 6. Calculation data are collected in Table 2.

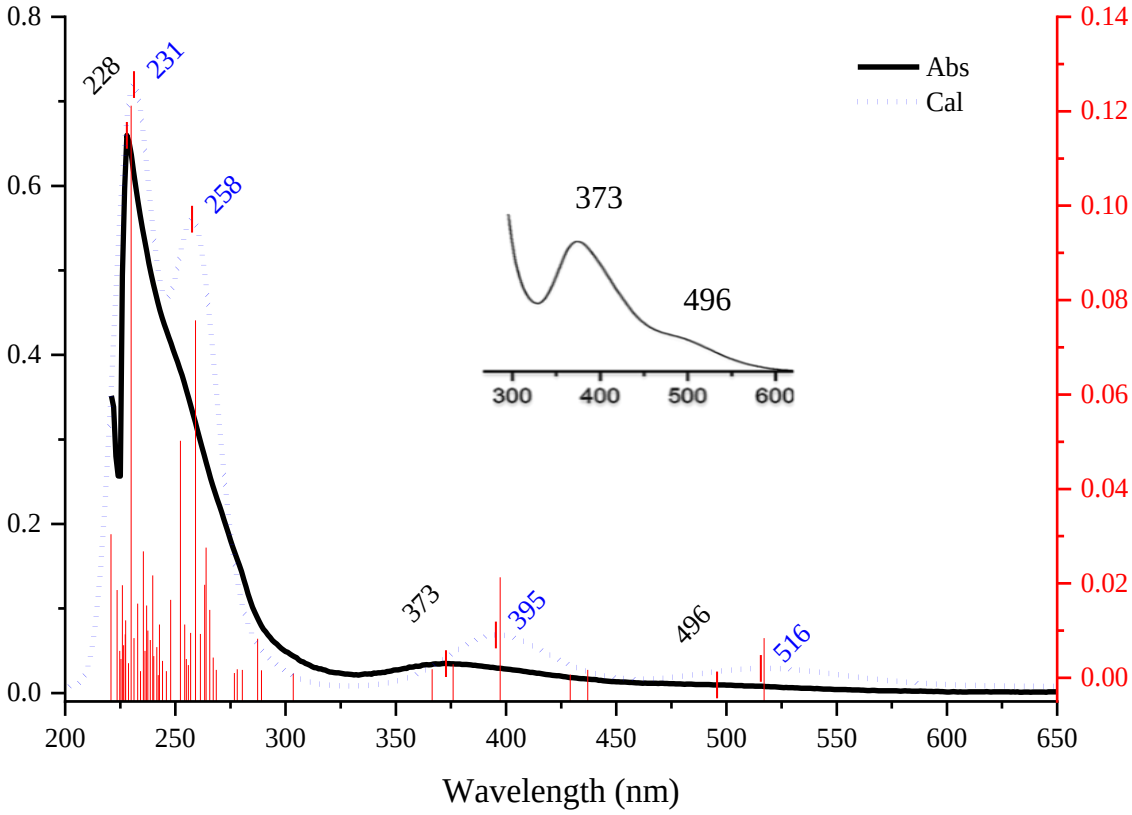

Figure 5 The UV– Visible absorption spectra overlaid with the PCM- TD- PBE0/ 6-31+ G* + LANL2DZ simulated spectra (dotted line) . Corresponding oscillator strengths are shown as sets of vertical lines.

Table 2 Photophysical data and vertical electronic transitions calculated for Ru(*p*-cymene)(PPh_3)Cl_2 complex.

No.	Wavelength (nm)		Osc. Strength (f)	Major contribution	Assignment
	Cal	Exp			
1	516	496 (sh)	0.0084	HOMO→LUMO (79%)	LLCT (PPh_3→*p*-cymene)
4	395	373	0.0213	HOMO→L+1 (65%)	MLCT, XLCT (Cl→PPh_3)
19	258	-	0.0757	H-5→L+1 (39%)	LLCT (PPh_3→*p*-cymene) LMCT (PPh_3→Ru)
41	231	228	0.1212	H-4→L+2 (18%) H-3→L+2 (42%)	XLCT (Cl→PPh_3)

sh = shoulder

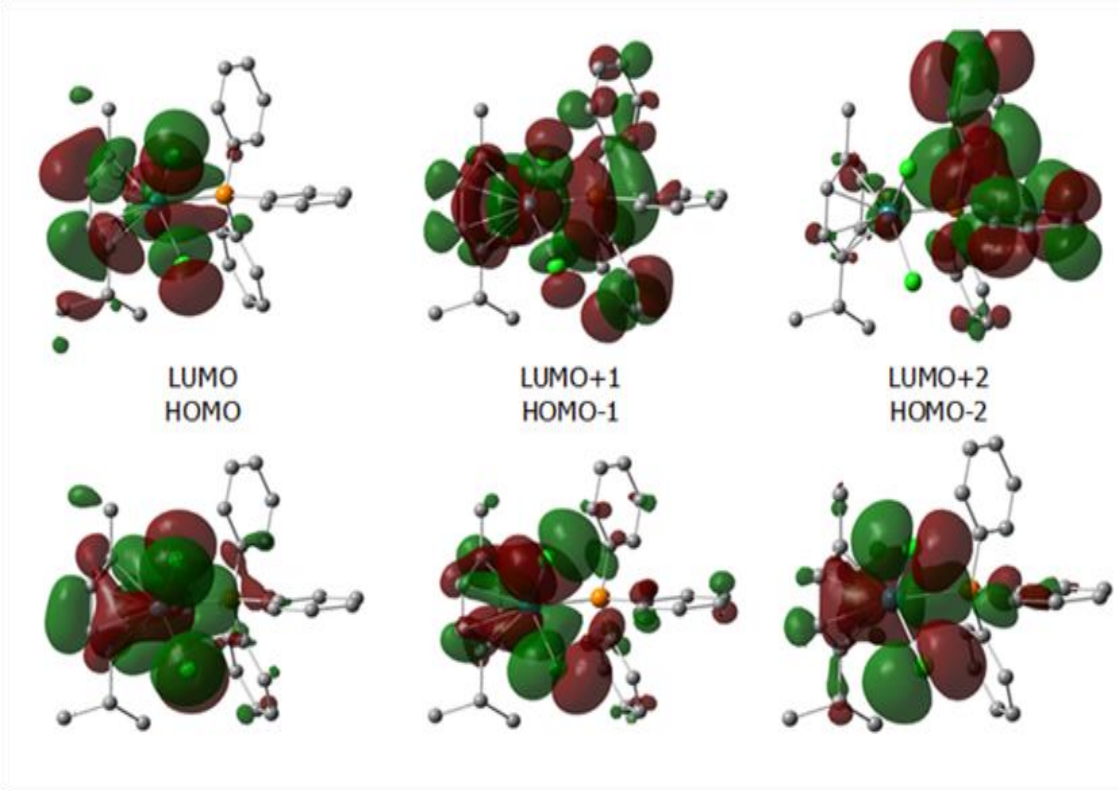

Figure 6 Contour plots of HOMO and LUMO molecular orbitals of the Ru (*p*-cymene)(PPh_3)Cl_2 complex.

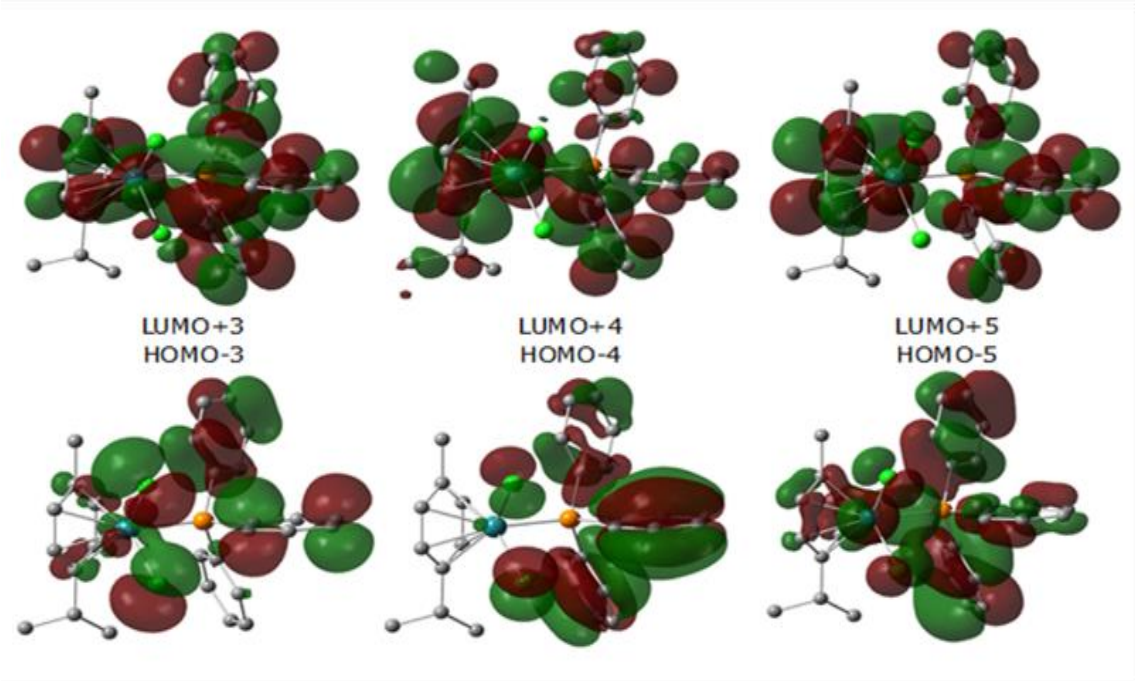

Figure 6 (continuous)

Anticancer activity

Figure 7 shows the plot of cell viability percentage against the tested concentration of Ru(*p*- cymene) (PPh_3) Cl_2 complex in the range 0. 01 to 100 µM respectively, for MCF- 7, HCC1937, and MDA- MB- 231 cell lines. The Ru(*p*-cymene)(PPh_3)Cl_2 complex showed the best activity for the *in vitro* cytotoxicity selectively against the MCF- 7 cell line, presenting an IC_{50} value of 15.99 µM, which showed better sensitivity than that of cisplatin and Phosphine (PPh_3) free ligand, as summarized in Table 3. For the other examined breast cancer cells, the IC_{50} values were all less sensitive than cisplatin, with concentration higher than 100 µM against those two cell lines. The result for MCF-7 corresponds to the report from Honorato *et al*. (2020). The presence of PPh_3 which is a lipophilic group, can increase the cellular uptake of the complex, influencing the cytotoxicity toward the cancer cell. Nevertheless, in order to explain selectivity to MCF- 7, further. for the possible mechanism of cancer cell inhibition.

Table 3 IC_{50} mean values (µM) against HCC1937, MCF-7 and MDA-MB-231 cells after 48 hrs of treatment.

Metal complex	**IC_{50} (µM)**		
	MCF-7	**HCC1937**	**MDA-MB-231**
Cisplatin	$42.2 \pm 8^{*,**}$	$23.4 \pm 7^{*,**}$	$128.2 \pm 7^{*,**}$
$RuPPh_3$	$15.99 \pm 5^{*,**}$	$>100^{*,**}$	$>100^{*,**}$
PPh_3	$>100^{*,**}$	$54.3 \pm 0.2^{*,**}$	$>100^{*,**}$

The following symbols represent statistically significant differences: $*\ p < 0.01$, compared to the IC_{50} values of the same complex on cell lines; and $**p > 0.001$, compared to the IC_{50} values of the complexes on each cell line.

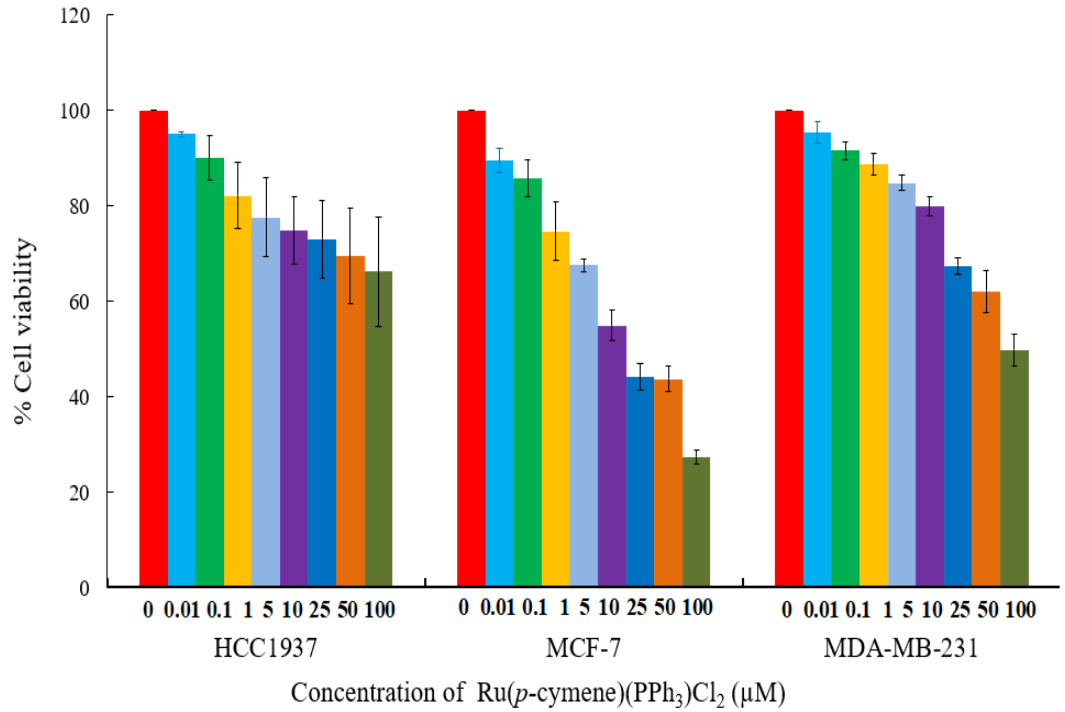

Figure 7 The chart shows the cytotoxic effect of Ru(*p*-cymene)(PPh3)Cl2 at concentrations of 0, 0.01, 0.1, 1, 5, 10, 25, 50, and 100 µM on the cell viability of HCC1937, MCF-7 and MDA-MB-231 cells after 48 hrs.

CONCLUSION

Single crystal x-ray diffraction, elemental analysis, and spectroscopy methods were used to analyze the Ru (*p*-cymene) (PPh3)Cl2 complex. The geometry of this complex adopts a distorted pseudo-tetrahedral. H-bonding is evident in both intramolecular and intermolecular interactions within the crystal structure. Density functional theory identified that the absorption band at 393 nm, with a shoulder of 496 nm, arises from the mixing character of charge transfer transitions. As a result of this investigation, the Ru(*p*-cymene)(PPh3)Cl2 complex was assessed for its cytotoxicity selectively against human breast cancer cell line MCF-7 a lower IC_{50} value than that of cisplatin.

ACKNOWLEDGMENT

NL would like to extend our sincere gratitude to the Royal Scholarship under Her Royal Highness Princess Maha Chakri Sirindhorn Education Project and the Graduate School, Prince of Songkla University, for providing Mr. Vannara Soem with the opportunity and financial support to pursue his master' s degree at the Division of Physical Science, Faculty of Science, Prince of Songkla University. We also thank the Ministry of Education and the Faculty of Science at PSU for their financial support, as well as the financial funding from the Center for Innovation in Chemistry (PERCH-CIC), the Commission on Higher Education.

REFERENCES

Allardyce, C. S. and Dyson, P. J. 2001. Ruthenium in medicine: current clinical uses and future prospects. **Platinum Metals Reviews** 45: 62.

Bergamo, A. and Sava, G. 2011. Ruthenium anticancer compounds: Myths and realities of the emerging metal-based drugs. **Dalton Transactions** 40(31): 7817-7823.

Biancalana, L., Zacchini, S., Ferri, N., Lupo, M.G., Pampaloni, G. and Marchetti, F. 2017. Tuning the cytotoxicity of ruthenium(II) para-cymene complexes by mono-substitution at a triphenylphosphine

/phenoxydiphenylphosphine ligand. **Dalton Transactions** 46(47) : 16589-16604.

Brissos, R. F. , Clavero, P. , Gallen, A. , Grabulosa, A., Barrios, L.A., Caballero, A. B. , Korrodi- Gregório, L. , Pérez-Tomás, R., Muller, G., Soto-Cerrato, V. and Gamez, P. 2018. Highly Cytotoxic Ruthenium(II)-Arene Complexes from Bulky 1- Pyrenylphosphane Ligands. **Inorganic Chemistry** 57(23): 14786-14797.

Chuklin, P., Chalermpanaphan, V., Nhukeaw, T., Saithong, S., Chainok, K., Phongpaichit, S., Ratanaphan, A. and Leesakul, N. 2017. Synthesis, X-ray structure of organometallic ruthenium(II) *p*-cymene complexes based on P- and N- donor ligands and their *in vitro* antibacterial and anticancer studies. **Journal of Organometallic Chemistry** 846: 242-250.

Dkhar, L., Banothu, V., Kaminsky, W. and Kollipara, M.R. 2020. Synthesis of half sandwich platinum group metal complexes containing pyridyl benzothiazole hydrazones: Study of bonding modes and antimicrobial activity. **Journal of Organometallic Chemistry** 914: 121225.

Elsegood, M.R.J., Smith, M.B. and Sanchez-Ballester, N.M. 2006. Dichloro(η^6-*p*-cymene)(triphenylphosphine) -ruthenium (II). **Acta Crystallographica Section E: Structure Reports Online** 62(11): 2838-2840.

Farrugia, L.J. 2012. WinGX and ORTEP for Windows: An update. **Journal of Applied Crystallography** 45(4): 849-854.

Govindaswamy, P., Mozharivskyj, Y.A. and Kollipara, M.R. 2004. New neutral and cationic η^6- arene ruthenium complexes with phosphine and amine ligands: Syntheses and molecular structures of [(η^6- *p*- cymene) Ru ($NH_2CH_2C_6$) H_5) Cl_2] , [(η^6-C_6Me_6) Ru(PPh_2Py) Cl_2] and [(η^6-C_6Me_6)Ru(PPh_2Py)Cl]$^+$. **Polyhedron** 23(18): 3115-3123.

Henry, B., Batchelor, L.K., Roufosse, B., Romano, D., Baumgartner, J., Borzova, M., Reifenstahl, T., Collins, T., Benamrane, A., Weggelaar, J., Correia, M.C., Dyson, P.J. and Blom, B. 2019. Heterobimetallic Ru(μ- dppm) Fe and homobimetallic Ru(μ-dppm)Ru complexes as potential anti- cancer agents. **Journal of Organometallic Chemistry** 901: 120934.

Honorato, J., Oliveira, K. M., Leite, C. M., Colina- Vegas, L. , Nóbrega, J. A. , Castellano, E.E., Ellena, J., Correa, R.S. and Batista, A. A. 2020. " Half-Sandwich"/Ru^{II} Anticancer Complexes Containing Triphenylphosphine and *p*-Substituted Benzoic Acids. **Journal of the Brazilian Chemical Society** 31: 2237-2249.

Klaimanee, E., Nhukeaw, T., Saithong, S., Ratanaphan, A., Phongpaichit, S., Tantirungrotechai, Y. and Leesakul, N. 2021. Half-sandwich ruthenium(II) *p*- cymene complexes based on organophosphorus ligands: Structure determination, computational investigation, *in vitro* antiproliferative effect in breast cancer cells and antimicrobial activity. **Polyhedron** 204: 115244.

Lapasam, A., Dkhar, L., Joshi, N., Poluri, K.M. and Kollipara, M.R. 2019. Antimicrobial selectivity of ruthenium, rhodium, and iridium half sandwich complexes containing phenyl hydrazone Schiff base ligands towards B. thuringiensis and P. aeruginosa bacteria. **Inorganica Chimica Acta** 484: 255-263.

Li, J., Tian, M., Tian, Z., Zhang, S., Yan, C., Shao, C. and Liu, Z. 2018. Half-sandwich iridium(III) and ruthenium(II) complexes containing P^P-chelating ligands: A new class of potent anticancer agents with unusual redox features. **Inorganic Chemistry** 57(4): 1705-1716.

Ludwig, G., Kaluđerović, G.N., Bette, M., Block, M. , Paschke, R. and Steinborn, D. 2012. Highly active neutral ruthenium(II) arene complexes: Synthesis, characterization, and investigation of their anticancer

properties. **Journal of Inorganic Biochemistry** 113: 77-82.

Mawnai, I.L., Adhikari, S., Dkhar, L., Tyagi, J.L., Poluri, K.M. and Kollipara, M.R. 2019. Synthesis and antimicrobial studies of half- sandwich arene platinum group complexes containing pyridylpyrazolyl ligands. **Journal of Coordination Chemistry** 72(2): 294-308.

MacRae, C.F., Sovago, I., Cottrell, S.J., Galek, P.T.A., McCabe, P., Pidcock, E., Platings, M., Shields, G.P., Stevens, J.S., Towler, M. and Wood, P.A. 2020. Mercury 4.0: From visualization to analysis, design and prediction. **Journal of Applied Crystallography** 53: 226-235.

Mennucci, B., Cancès, E. and Tomasi, J. 1997. Evaluation of solvent effects in isotropic and anisotropic dielectrics and in ionic solutions with a unified integral equation method: Theoretical bases, computational implementation, and numerical applications. **Journal of Physical Chemistry B** 101(49): 10506-10517.

Murray, B.S., Babak, M.V., Hartinger, C.G. and Dyson, P.J. 2016. The development of RAPTA compounds for the treatment of tumors. **Coordination Chemistry Reviews** 306: 86-114.

Neethu, K.S., Eswaran, J., Theetharappan, M., Nattamai S.P.B., Neelakantan, M.A. and Velusamy, K. M. 2019. Organoruthenium(II) complexes featuring pyrazole-linked Schiff base ligands: Crystal structure, DNA/ BSA interactions, cytotoxicity and molecular docking. **Applied Organometallic Chemistry** 33(3): 1-16.

Orhan, E., Dülger, G., Alpay, M., Öksüz, N. and Dülger, B. 2022. Synthesis, antimicrobial and antiproliferative activities of new self- assembly benzimidazole-bridged aren ruthenium rectangles in human breast cancer cells. **Journal of Inclusion Phenomena and Macrocyclic Chemistry** 102(1-2): 45-54.

Pettinari, R., Pettinari, C., Marchetti, F., Skelton, B.W., White, A.H., Bonfili, L. and Eleuteri, A.M. 2014. Arene-ruthenium (II) acylpyrazolonato complexes: apoptosis-promoting effects on human cancer cells. **Journal of medicinal chemistry** 57(11): 4532-4542.

Rohini, G., Haribabu, J., Aneesrahman, K.N., Bhuvanesh, N.S.P., Ramaiah, K., Karvembu, R. and Sreekanth, A. 2018. Half-sandwich Ru(II) (η^6-*p*-cymene) complexes bearing N-dibenzosuberenyl appended thiourea for catalytic transfer hydrogenation and *in vitro* anticancer activity. **Polyhedron** 152: 147-154.

Rojas, S., Carmona, F.J., Barea, E. and Maldonado, C.R. 2017. Inorganic mesoporous silicas as vehicles of two novel anthracene- based ruthenium metalloarenes. **Journal of Inorganic Biochemistry** 166: 87-93.

Roy, L.E., Hay, P.J. and Martin, R.L. 2008. Revised basis sets for the LANL effective core potentials. **Journal of Chemical Theory and Computation** 4(7): 1029-1031.

Sáez, R., Lorenzo, J., Prieto, M.J., Font-Bardia, M., Calvet, T., Omeñaca, N., Vilaseca, M. and Moreno, V. 2014. Influence of PPh_3 moiety in the anticancer activity of new organometallic ruthenium complexes. **Journal of Inorganic Biochemistry** 136: 1-12.

Sheldrick, G.M. 2015. Crystal structure refinement with SHELXL. **Acta Crystallographica Section C: Structural Chemistry** 71: 3-8.

Spackman, P.R., Turner, M.J., McKinnon, J.J., Wolff, S.K., Grimwood, D.J., Jayatilaka, D., and Spackman, M.A. 2021. CrystalExplorer: A program for Hirshfeld surface analysis, visualization, and quantitative analysis of molecular crystals. **Journal of Applied Crystallography** 54(3): 1006-1011.

Subarkhan, M.K.M. and Ramesh, R. 2016. Ruthenium(II) arene complexes containing benzhydrazone ligands: Synthesis, structure and antiproliferative activity.

Inorganic Chemistry Frontiers 3(10): 1245-1255.

Tabares, J.P.G., Santos, R.L.S.R., Cassiano, J.L., Zaim, M.H., Honorato, J., Batista, A.A., Teixeira, S.F., Ferreira, A.K., Viana, R.B., Martínez, S.Q., Stábile, A.C. and de Oliveira Silva, D. 2019. A Ru(II) - *p*- cymene compound bearing naproxen-pyridineamide. Synthesis, spectroscopic studies, computational analysis and *in vitro* anticancer activity against lung cells compared to Ru(II) - *p*- cymene-naproxen and the corresponding drug ligands. **Inorganica Chimica Acta** 489: 27-38.

Yellol, J., Pérez, S.A., Buceta, A., Yellol, G., Donaire, A., Szumlas, P., Bednarski, P.J., Makhloufi, G., Janiak, C., Espinosa, A. and Ruiz, J. 2015. Novel C,N-Cyclometalated Benzimidazole Ruthenium(II) and Iridium(III) Complexes as Antitumor and Antiangiogenic Agents: A Structure-Activity Relationship Study. **Journal of Medicinal Chemistry** 58(18): 7310-7327.

Zeng, L., Gupta, P., Chen, Y., Wang, E., Ji, L., Chao, H. and Chen, Z.S. 2017. The development of anticancer ruthenium(II) complexes: From single molecule compounds to nanomaterials. **Chemical Society Reviews** 46(19): 5771-5804.